Fracture Toughness and Failure Mechanisms of Epoxy/Rubber-Modified Polystyrene (HIPS) Interfaces Reinforced by Grafted Chains

Y. Sha and C. Y. Hui*

Department of Theoretical and Applied Mechanics and the Materials Science Center, Cornell University, Ithaca, New York 14853

E. J. Kramer*

Department of Materials Science and Engineering and the Materials Science Center, Cornell University, Ithaca, New York 14853

S. F. Hahn and C. A. Berglund

Central Research and Development, Dow Chemical Company, Midland, Michigan 48674

Received December 5, 1995[⊗]

ABSTRACT: The fracture toughness G_c of epoxy/high-impact polystyrene (HIPS) interfaces was measured as a function of grafting chain density Σ of carboxylic acid terminated deuterated polystyrene (dPS-COOH) chains of various degrees of polymerization N. The dPS chains penetrate into the bulk HIPS whereas the −COOH end functional group is chemically bonded to the epoxy. For short chains, e.g., $N = 160$, no effective entanglements can be formed between the dPS chains and the PS matrix of the HIPS, and thus no enhancement in G_c over that of a bare interface. For longer chains, $N = 410$, the interface fails by chain pullout from the PS matrix of HIPS at low Σ. There is a transition from chain pullout to crazing above an areal chain density $\Sigma^{\dagger} \approx 0.025$ chains/nm^2 at this chain length. For very long chains, e.g., $N = 1860$, even though each chain is well entangled, the maximum grafting density achievable is very low and such an interface fails by scission of the chains so that the interface fracture toughness is also low. Large values of G_c are observed at intermediate chains lengths where both effective entanglements can be formed and a large Σ can be achieved. Under these conditions, the interface fails initially due to the formation of crazes in the HIPS side of the interface and the subsequent breakdown of one of these crazes at the interface. As Σ increases, the mechanism of interface failure undergoes a transition from scission of the bridging chains before craze formation to a mechanism where crazing occurs and is followed by craze failure. The critical areal chain density at which this transition occurs, Σ_c, is independent of N and is found to be ∼0.015 chains/nm^2 for the epoxy/HIPS system. The maximum grafting density achievable is observed to decrease linearly with increasing N, and the optimum interface adhesion appears to be achieved with N around 1000. The results are compared with those of epoxy/PS interfaces for which the PS has a higher crazing stress and thus a higher $\Sigma_c \sim 0.03$ chains/nm^2.

1. Introduction

Polymer additives, often called compatibilizers, are widely used to reinforce interfaces between immiscible polymers. One class of compatibilizers consists of the diblock copolymers,[1−6] a block of polymer miscible with polymer 1 joined covalently to a block of polymer miscible with polymer 2. The block copolymer chains form interphase junctions through which stress can be transferred, thus resulting in substantial reinforcement of the interfaces. The interaction between the block copolymer and the homopolymers can be either via van der Waals bonds[4,5] or via hydrogen bonds,[6,7] but present evidence suggests that entanglement, rather than the details of intermolecular bonding plays a dominant role.[7] Another class of compatibilizers are additives[8,9] which dissolve in phase 1 but chemically react with phase 2 to form a graft copolymer at the interface. A review of what is known about both types of reinforcement can be found in ref 10.

In this work, we studied the interface between a cross-linked epoxy thermoset and high-impact polystyrene (HIPS). This interface was reinforced using deuterated polystyrene chains terminated with carboxylic acid groups (dPS-COOH). The dPS chains penetrate into the bulk high-impact polystyrene whereas the −COOH end reacts with the epoxy to form a chemical bond. The interface adhesion is quantified by determining the interface fracture toughness G_c, which is measured by the asymmetric double cantilever beam (ADCB) technique.[11−13] After fracture, forward-recoil spectrometry (FRES) is used to measure the amount of deuterium on each side of the interface. Since deuterium is used to label the grafted chains, the sum of the deuterium on the two surfaces could be used to determine the areal chain density, Σ, of the grafted polymer at the interface. By analyzing the ratio of deuterium on the epoxy side after fracture to the total deuterium, Σ_{ep}/Σ, we also gain important information about the interface failure mechanism. We study the effect of the degree of polymerization, N, of the dPS chains and the grafting areal density, Σ, on G_c. To observe the effect of placing −COOH randomly along the dPS chain rather than only at the end, we investigated the effect of one dPS with randomly distributed −COOH functional groups for reinforcing the interface between HIPS and epoxy. These results are compared with those for epoxy/PS interfaces reinforced with the same dPS-COOH chains.[9]

The fracture mechanism map[14] displayed in Figure 1 shows that the normal stress that can be borne by the

[⊗] Abstract published in *Advance ACS Abstracts,* May 15, 1996.

S0024-9297(95)01794-3 CCC: $12.00 © 1996 American Chemical Society

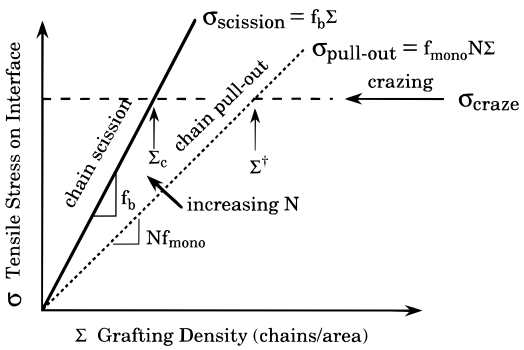

Figure 1. Fracture mechanism map.

interface before the chains bridging the interface break is

$$\sigma_{\text{scission}} = f_b\Sigma \tag{1}$$

where f_b is the force to break a backbone bond in the chain. When σ_{scission} reaches the value of the crazing stress, σ_{craze}, which is independent of areal chain density, there is a transition from a mechanism of interface failure by scission of the bridging chains prior to crazing to a mechanism of crazing followed by craze failure. This transition areal density, Σ_c, is given by

$$\Sigma_c = \sigma_{\text{craze}}/f_b \tag{2}$$

Note that Σ_c is independent of N, the degree of polymerization.

The transition from chain scission to crazing occurs only when the slope of the chain pull-out curve, i.e., $f_{\text{mono}}N$ is greater than f_b. Thus, pullout will not occur when the grafting chains are sufficiently long. On the other hand, when the interface is modified with short grafted chains, so that $f_{\text{mono}}N < f_b$, the interface will fail by pullout of the grafted chains from the thermoplastic when a stress, σ_{pullout}, is reached. This is shown in Figure 1, where the pullout mechanism is represented by a line with slope $f_{\text{mono}}N$. σ_{pullout} is the stress required to pull out the grafted chains, i.e.

$$\sigma_{\text{pullout}} = f_{\text{mono}}N\Sigma \tag{3}$$

The increment of the interface fracture toughness ΔG_c above that of the bare interface increases as $\Delta G_c \propto N^2\Sigma$.[12,24] Experimentally, ΔG_c is nearly independent of crack velocity over the range 1×10^{-7} to 1×10^{-4} m/s, so f_{mono} can be interpreted as a static monomer friction. As shown in Figure 1, for these short grafting chains, there is a transition from chain pullout to crazing when the areal chain density reaches

$$\Sigma^\dagger = \sigma_{\text{craze}}/(f_{\text{mono}}N) \tag{4}$$

2. Experiment

2.1. Materials. The epoxy resin, consisting of the diglycidyl ether of Bisphenol A, had a molar mass of 350 g/mol. Triethylenetetramine (TETA) is used as cross-linker. The HIPS, containing 8.48% by weight of polybutadiene rubber, *ca.* 1.2 μm in diameter, was provided by the Dow Chemical Co.; the PS matrix had a weight-average molecular weight of 232 500 and a number-average molecular weight of 88 730. The HIPS contained 0.14% by weight of an antioxidant but did not contain any plasticizers, mold release agents, or other additives that could diffuse to and weaken an interface. The carboxylic acid terminated deuterated polystyrene (dPS-COOH) was prepared using anionic polymerization. Details of the polymerization and termination procedure can be found in ref 9. The degree of polymerization of the dPS chains N, the weight-average molecular weights M_w, and the polydispersity indices M_w/M_n for the dPS-COOH samples are listed in Table 1.

Chains of dPS with a few phenyl groups randomly carboxylated in the para position were also explored. The degree of polymerization of the dPS chain was 700 and its polydispersity index was 1.08, with 1% of the phenyl rings functionalized. This means on average there is one carboxylic acid group every 100 monomer units, or about 6 acid groups per chain, with an additional acid group at the terminal end of each chain. This polymer was prepared using the method reported by Hird and Eisenberg;[15] dPS was subjected to Friedel−Crafts acylation with acetyl chloride in carbon disulfide, followed by haloform oxidation of the acetyl groups to carboxylic acid groups.

2.2. Sample Preparation. The epoxy resin was heated up to 45 °C for 0.5 h to form a melt and then mixed with TETA for 2−17 min. The stoichiometry S, which is defined as the ratio of amine hydrogens to epoxide groups in the mixture, was held constant at 1.5. The mixture was then injected into a glass sandwich mold using poly(tetrafluoroethylene) (PTFE) as a spacer. The glass surface was coated with a self-assembled monolayer[16] of octadecyltrichlorosilane (OTS) to prevent the glass from sticking to the epoxy plate. The epoxy moled was then transferred to an oven to carry out a B-stage cure in air at a temperature between 80 and 120 °C for 2 h. After the epoxy was removed from the mold, a 2% solution of dPS-COOH in toluene was spun cast onto the epoxy surface for 40 s, producing a pure dPS-COOH film about 900 Å thick on the epoxy. For the bare interface sample, only pure toluene solvent was spun cast onto the epoxy. The dPS-coated epoxy slab was then annealed at 160 °C under vacuum for 6 h to allow the dPS-COOH chains to react with the epoxy network. An entropic barrier to the grafting reaction is thought to determine the kinetics of grafting and thus the areal chain density of dPS that is grafted onto the epoxy.[17] The unreacted chains were removed by washing the epoxy slab in tetrahydrofuran (THF) in an ultrasonic bath for 20 min. The epoxy slab was then dried at 80 °C for 2 h under vacuum.

The HIPS slab was made by compression molding at 160 °C. The epoxy plate was then joined to the HIPS slab at 160 °C under contact pressure for 2 h to allow the tails of the grafted dPS chains to entangle with the HIPS. The sandwich was then cooled to room temperature in air and cut into strips 50 mm long and 9 mm wide. The thicknesses of the epoxy and HIPS strips were 0.8 and 1.6 mm, respectively.

The areal density of deuterium atoms N_D presented on each of the two fracture surfaces was measured by forward-recoil spectrometry (FRES). The $^4He^{2+}$ beam energy used was 2.75 MeV. The areal density of chains Σ was then calculated by dividing N_D by the number ($8N$) of deuterium atoms per chain.

2.3. Fracture Toughness Measurement. The asymmetric double cantilever beam (ADCB) fracture specimen is shown schematically in Figure 2. The fracture toughness measurement was performed by driving a single-edged razor blade, of thickness Δ, along the interface at a constant rate of 3×10^{-6} m/s using a servomotor driver. The fracture toughness of the interface G_c is given by the critical energy release rate of the interfacial crack. The energy release rate G was computed using[12]

$$G = \frac{3\Delta^2 E_{ep} h_{ep}^3 E_{hp} h_{hp}^3}{8a^4}\left[\frac{E_{ep}h_{ep}^3 C_{hp}^2 + E_{hp}h_{hp}^3 C_{ep}^2}{(E_{ep}h_{ep}^3 C_{hp}^3 + E_{hp}h_{hp}^3 C_{ep}^3)^2}\right] \tag{5}$$

In eq 5, h_{hp} and E_{hp} denote the thickness and the Young's modulus of the HIPS slab and $C_{hp} = 1 + 0.64h_{hp}/a$. The quantities C_{ep}, E_{ep}, and h_{ep} are similarly defined for epoxy and are labeled by the subscript ep. The crack length a is measured from the crack tip to the edge of the razor blade. To allow many measurements of a and thus G_c to be made, the entire history of the crack growth was recorded using a videocamera and a videotape was recorded for subsequent playback and measurement.

Table 1

N	160	410	540	690	840	1290	1480	1790
M_w	16 600	42 900	55 700	71 500	87 100	134 900	153 700	186 000
M_w/M_n	1.03	1.02	1.04	1.07	1.1	1.1	1.06	1.2

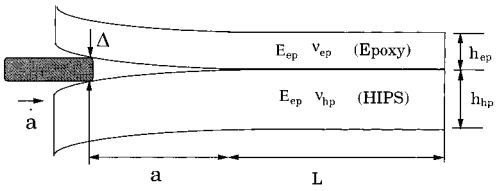

Figure 2. Asymmetric double cantilever beam fracture specimen for the HIPS/epoxy system.

2.4. Fracture Mechanics. The mechanics of fracture along a bimaterial interface has been studied extensively. Excellent reviews can be found in refs 18−20. The stress and deformation field near the tip of a crack lying along a bimaterial interface can be uniquely characterized by means of the complex stress intensity factor $K = K_1 + iK_2$,[18] where $i = (-1)^{1/2}$. K_1 and K_2 have dimensions of (Pa $m^{1/2-i\epsilon}$) and are functions of the sample geometry, applied loading, and material properties. In experiments, it is easier to measure the energy release rate G, which is related to K by

$$G = C|K|^2/[16\cosh^2(\pi\epsilon)] \tag{6a}$$

where

$$\epsilon = \frac{1}{2\pi}\ln\left(\frac{\frac{\kappa_{ep}}{\mu_{ep}} + \frac{1}{\mu_{hp}}}{\frac{\kappa_{hp}}{\mu_{hp}} + \frac{1}{\mu_{ep}}}\right)$$

and

$$C = \frac{\kappa_{ep} + 1}{\mu_{ep}} + \frac{\kappa_{hp} + 1}{\mu_{hp}}$$

Here $\kappa_i = 3-4\nu_i$ for plane strain and $(3 - \nu_i)/(1 + \nu_i)$ for plane stress and where ν_i and μ_i are the Poisson's ratio and the shear modulus of material i. For the epoxy/HIPS system, the shear moduli and Poisson's ratios for the two materials are $\mu_{hp} = 0.776$ GPa, $\mu_{ep} = 1.306$ GPa, and $\nu_{hp} = \nu_{ep} = 0.34$. ϵ is found to be -0.0197 for interfaces under plane strain conditions.

Since G is real, an additional dimensionless quantity, the phase angle ψ, is needed to fully specify the crack tip stress field, where ψ is defined by

$$\exp(i\psi) = (Kd^{i\epsilon})/|K| \tag{6b}$$

The choice of the characteristic length d is arbitrary.[18] For the epoxy/HIPS system, d is chosen to be 100 μm as in the PS/PVP system.[4] Note that, for the special case of $\epsilon = 0$, K_1 and K_2 become the classical tensile (mode I) and shear (mode II) stress intensity factors K_I and K_{II}. For this special case, ψ is the tensile and shear mode mixity at the crack tip; i.e., $\psi = \tan^{-1}(K_{II}/K_I)$.

It is important to control the phase angle in our experiments so that the crack stays at the interface. For example, the measured G_c increases significantly as the ratio of the epoxy slab thickness to that of the HIPS slab increases (see ref 21). In our experiments, the thickness of the HIPS slab is chosen to be twice that of the epoxy slab so the crack is driven to the epoxy slab and any craze nucleated from the interface ahead of the crack tip will be oriented at $-135°$ to the crack growth directions.[4] Since the yield stress of epoxy is much higher than the crazing stress of HIPS, this choice of thickness allows the crack tip to stay along the interface while minimizing craze formation in the HIPS and plastic deformation in the epoxy. The phase angle ψ for the ADCB specimen used in our experiments was determined to be $-16°$ using a finite element method. This phase angle also compares well with that obtained by a boundary element method which has been reported.[13] The boundary element method was also used to verify the validity of eq 5 for the geometry of our ADCB specimen and the typical crack lengths obtained in practice.

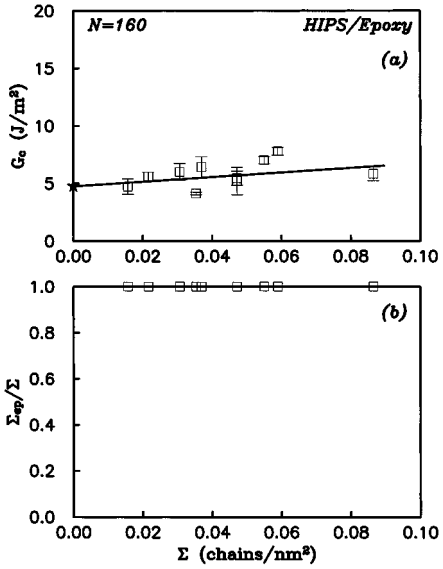

Figure 3. (a) Fracture toughness vs areal chain density for $N = 160$. (b) Fraction of deuterium on epoxy side after fracture for $N = 160$.

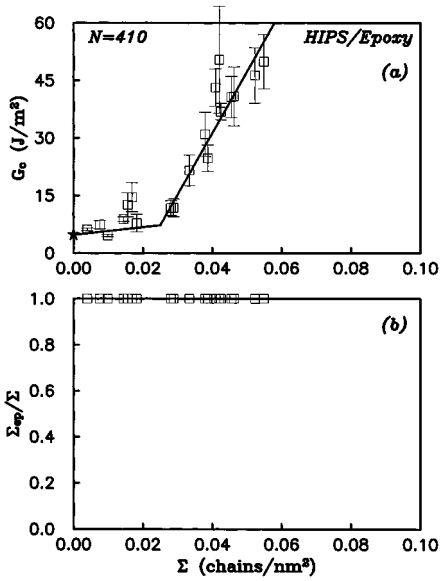

Figure 4. (a) Fracture toughness vs areal chain density for $N = 410$. (b) Fraction of deuterium on epoxy side after fracture for $N = 410$.

2.5. Thermal Residual Stresses. The thermal expansion coefficient of epoxy is 65×10^{-6} K^{-1} [22] and the measured thermal expansion coefficient of HIPS is 110×10^{-6} K^{-1}. This means that residual stresses due to the thermal expansion coefficient mismatch between HIPS and epoxy interface may affect the energy release rate calculation in eq 5, which was derived assuming no thermal stresses. Indeed our calculation in the appendix shows that an additional term must be appended to the energy release rate G given by eq 5; i.e., the energy release rate G^* of an ADCB sample subjected to both

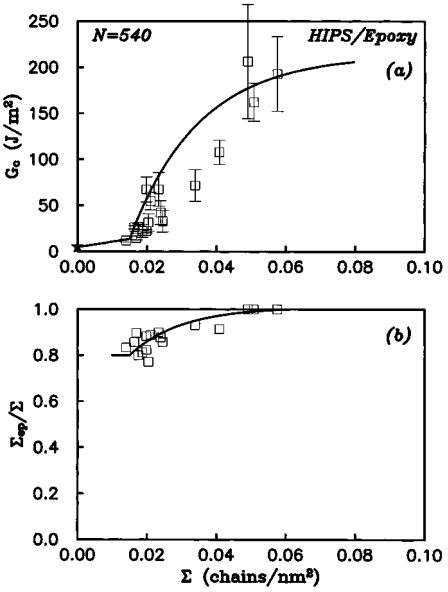

Figure 5. (a) Fracture toughness vs areal chain density for $N = 540$. (b) Fraction of deuterium on epoxy side after fracture for $N = 540$.

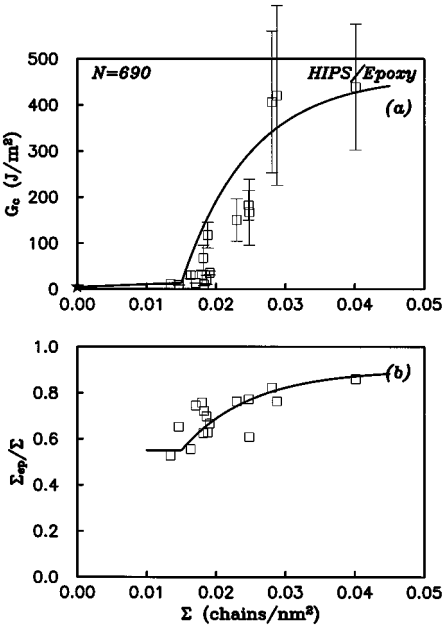

Figure 6. (a) Fracture toughness vs areal chain density for $N = 690$. (b) Fraction of deuterium on epoxy side after fracture for $N = 690$.

thermal and mechanical loading is

$$G^* = G + G_T \tag{7}$$

where G is given by eq 5 and G_T is the contribution due to thermal residual stresses, which is given by eq A9 in the appendix.

The measured differential scanning calorimetry (DSC) glass transition temperatures for HIPS and epoxy are 106 and 120 °C, respectively. Thus, even though the samples were prepared at 160 °C, the thermal stresses will only accumulate significantly at temperatures below about 100 °C, corresponding to the T_g of the PS matrix of the HIPS. The calculated G_T term for the bare interface, for which the thermal residual stresses are expected to have the biggest influence on the total energy release rate, is about 1 J/m^2. This is within our experimental error, which means we can neglect the effect of thermal residual stresses.

To further investigate the effect of thermal stresses, we carried out separate experiments using a fracture sample

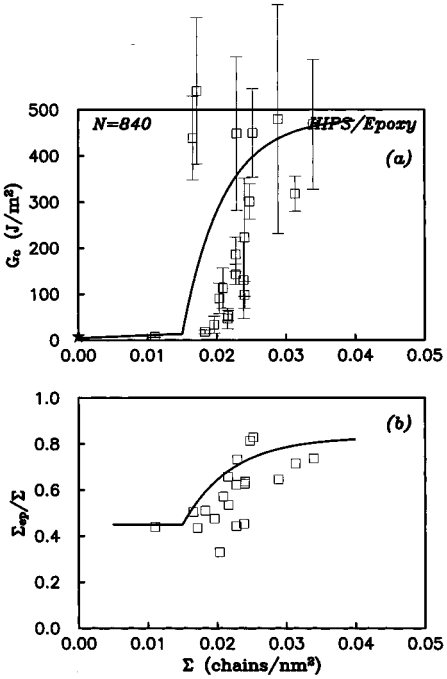

Figure 7. (a) Fracture toughness vs areal chain density for $N = 840$. (b) Fraction of deuterium on epoxy side after fracture for $N = 840$.

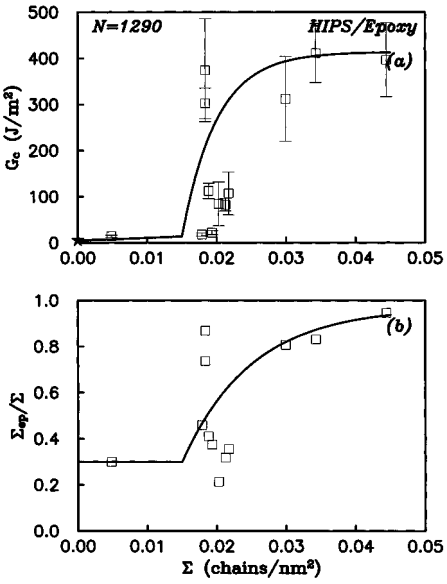

Figure 8. (a) Fracture toughness vs areal chain density for $N = 1290$. (b) Fraction of deuterium on epoxy side after fracture for $N = 1290$.

consisting of HIPS, PS, and epoxy. The PS in the sample is sandwiched between HIPS and epoxy. The thicknesses of HIPS and epoxy are 3.2 and 1.6 mm, respectively. The thickness of PS is about 0.2 mm, which is much smaller than that of the epoxy. Our experimental results indicate a negligible effect of thermal residual stresses on G, since the fracture toughness of the HIPS/PS/epoxy interface calculated using eq 5 is 4.1 J/m^2. This is essentially identical to the value obtained by Norton et al.,[9] who investigated the fracture toughness of PS/epoxy interfaces, for which thermal stresses can be ignored. The detailed analysis of the thermal residual stresses is given in the appendix.

3. Results

Plots of fracture toughness G_c versus interface areal chain density Σ for grafted dPS-COOH chains with different polymerization indices N are shown in Figures

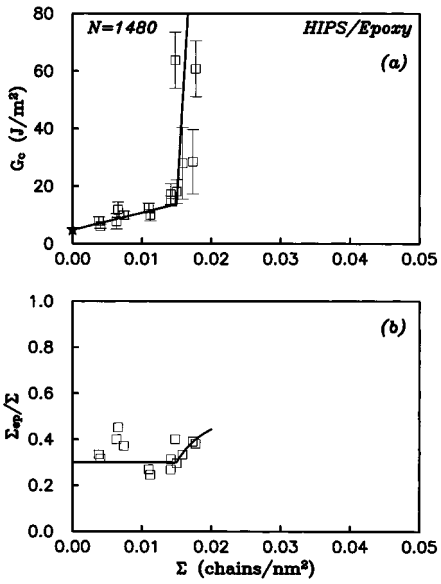

Figure 9. (a) Fracture toughness vs areal chain density for $N = 1480$. (b) Fraction of deuterium on epoxy side after fracture for $N = 1480$.

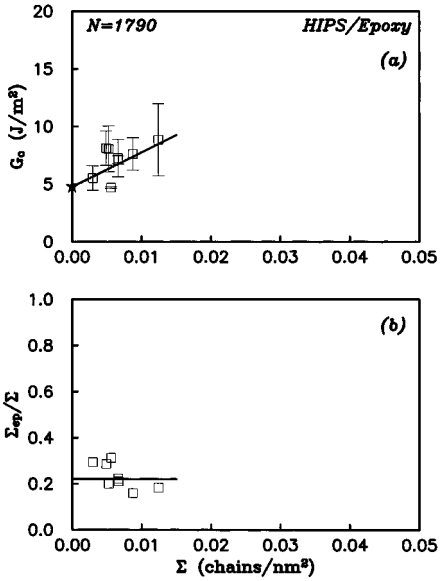

Figure 10. (a) Fracture toughness vs areal chain density for $N = 1790$. (b) Fraction of deuterium on epoxy side after fracture for $N = 1790$.

3a−11a. The corresponding plots of the fraction of deuterium found on the epoxy side versus areal chain density for the grafted dPS-COOH chains are shown in Figures 3b−11b. The fracture toughness of the bare interface is found to be 4.8 ± 0.5 J/m^2 and is shown as a star in Figures 3a−11a. Each data point on the fracture toughness curves in Figures 3a−11a is obtained by averaging 16 measurements. The error bars in these figures correspond to the standard deviation.

Short Chains ($N = 160$). The entanglement length N_e for PS is 173.[23] Thus for $N = 160$ practically no effective entanglements can be formed between the dPS chains and the PS matrix of HIPS. In Figure 3a the observed fracture toughness for the interface reinforced using $N = 160$ dPS-COOH chains is only slightly higher than that of the bare interface and is nearly independent of Σ. Postfracture FRES analysis Figure 3b shows that all the dPS is found on the epoxy side of the fracture surface, which clearly demonstrates that the interface fails by pullout of the dPS chains from the

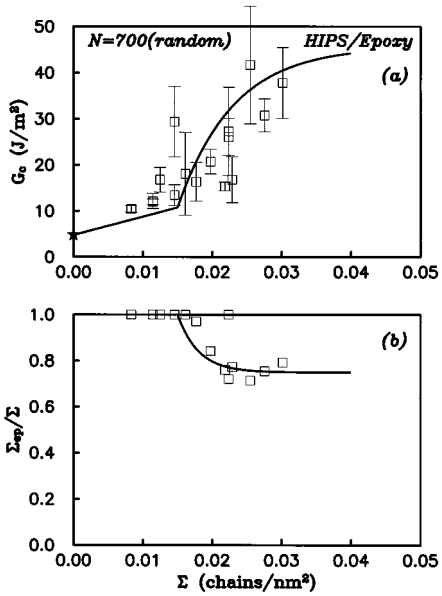

Figure 11. (a) Fracture toughness vs areal chain density for $N = 700$ (random dPS-COOH chain). (b) Fraction of deuterium on epoxy side after fracture for $N = 700$ (random).

HIPS side of the interface. This result agrees well with the expectation that when chains are not sufficiently entangled to provide stress transfer across the interface, there will be little increase in G_c over that of the bare interface, despite the fact that large grafting densities Σ can be reached.

Long Chains ($N = 1790$). The kinetics of grafting dPS chains with −COOH functional groups onto epoxy can be considered by two cases,[17] i.e., a case where the grafting is controlled by diffusion of free end-functional chains through the "brush" of previously grafted chains and a case where the grafting is controlled by the kinetics of the interface reaction itself. The rate of grafting of the two cases has the same form[17]

$$\frac{d\Sigma}{dt} = A \exp\left(-\frac{\mu^*(\xi)}{k_B T}\right) \tag{8}$$

$$A = \frac{D\rho_0}{a_0 N} \quad \text{for the diffusion case} \tag{8a}$$

and

$$A = \frac{a_0 k_f [C] \rho_0}{N} \quad \text{for the reaction case} \tag{8b}$$

where μ^* is the free energy of a free end-functional chain that has penetrated the brush and has its reactive end positioned adjacent to the interface but has not yet reacted; μ^* is a function of the single variable $\xi = N\Sigma/(\rho_0 R_g)$. ρ_0 is the segment density of the dPS-COOH polymer, R_g is the radius of gyration, N is the chain length, and Σ is the grafting density. a_0 in eq 8a is the statistical segment length, and the reaction is assumed to occur within a distance of a_0. D is the self-diffusion coefficient, and k_f in eq 8b is a (second order) rate constant. [C] is the concentration of groups in the epoxy that can react with dPS-COOH chains in the interfacial layer. $\mu^*/(k_B T)$ increases with N at a constant Σ. Since the grafting rate decreases exponentially with $\mu^*/(k_B T)$, the value of Σ at long times reaches a practical limit, and this limit strongly depends on N.

For long chains, the maximum areal chain density achievable at the interface is low and thus we expect the fracture toughness to be low, even though the anchored chains are well entangled with HIPS. For $N = 1790$, as shown in Figure 10a, the interface fracture toughness is close to that of the bare interface because the maximum areal chain density that can be reached for this case is only 0.014 chains/nm^2. The interface fails by chain scission of the dPS-COOH chains near the −COOH anchoring group prior to crazing. The deuterium distribution in Figure 10b shows that about 20% of the deuterium is left on the epoxy surface after fracture. This amount of deuterium can be explained by the penetration of dPS chains into the epoxy so that the −COOH end-functional group is grafted some distance below the epoxy surface.[9] Since the crack propagates along the epoxy/HIPS interface, this result implies that a length of about 300−400 dPS monomers on average is left on the epoxy.

Chain Scission to Crazing Transition ($N = 1480$). The fracture mechanism map in Figure 1 suggests that at low Σ the interface fails by scission of the grafted dPS chain. At higher Σ there should be a critical areal chain density Σ_c where the transition occurs from chain scission to crazing. This prediction is well supported by Figure 9a for $N = 1480$, which shows a sharp increase in G_c at $\Sigma_c \approx 0.015$ chains/nm^2. Using $f_b = 2 \times 10^{-9}$ N/bond[12] in eq 2, this result implies that the crazing stress of HIPS is ∼30 MPa, significantly lower than the crazing stress of PS (∼55 MPa) under the same conditions.

Chains of Intermediate Length ($N = 540$, 690, 840, and 1290). For short chain lengths, the maximum areal chain density that can be grafted on the interface is high (∼0.09 chains/nm^2) but the fracture toughness is low due to poor entanglement between the grafted chains and HIPS. In contrast, for very long grafted chains, the chains are well entangled with the PS matrix of HIPS but the maximum grafting density that can be achieved is low due to the slow kinetics of grafting.[17] Therefore we anticipate that the fracture toughness for intermediate chain lengths will be the highest. Figures 5a−8a show that the interface fracture toughness G_c for the intermediate chain lengths is low until a value of $\Sigma > \Sigma_c \approx 0.015$ chains/nm^2 is exceeded, upon which the G_c increases rapidly with further increases in Σ, eventually achieving a value as high as *ca.* 500 J/m^2, which is almost 100 times that of the bare interface, for $N = 840$ and 1290. This result also supports the prediction of the fracture mechanism map that Σ_c is independent of N.

The companion plots in Figures 5b−8b show the fraction of dPS found on the epoxy side after fracture. For $\Sigma < 0.015$ chains/nm^2, the fraction of dPS found on the epoxy side decreases strongly with N as shown in Figure 12. Forward-recoil spectrometry and neutron reflectivity suggest that the −COOH group may react at a distance somewhat below the surface of the epoxy.[9] From the data obtained, we assume that on average there are $N' = 220$ dPS monomer units embedded into the epoxy, and chain scission occurs at an additional $N'' = 180$ dPS units from the interface toward the HIPS (N'' is approximately the length between entanglements). Using these assumptions, the deuterium fraction on the epoxy side after fracture is given by

$$\Sigma_{ep}/\Sigma = (N' + N'')/N \qquad (9)$$

The percentage of deuterium on the epoxy side of the fracture in the low areal chain density regime from Figures 3b−10b is shown as the open circles in Figure 12. The solid line in Figure 12 is a plot of eq 9 with the assumed values of N' and N''. The fit to the data is excellent, supporting strongly the idea that a length of $N' \sim 220$ dPS is buried beneath the interface in the epoxy.

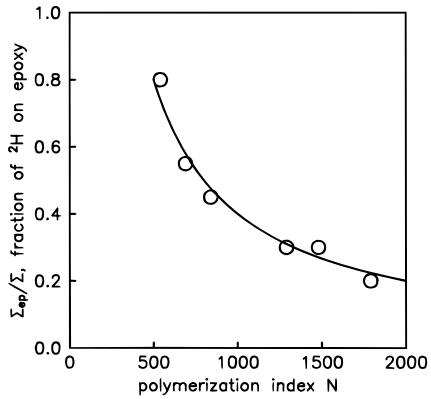

Figure 12. Fraction of deuterium on the epoxy side of the fracture in the low areal chain density ($\Sigma < 0.015$ chains/nm^2) regime versus the polymerization index of the dPS-COOH. The solid line is a plot of eq 9 for $N' = 220$ and $N'' = 180$.

As in the case of $N = 1480$, there is a transition from chain scission to crazing at $\Sigma = \Sigma_c \approx 0.015$ chains/nm^2. This assertion is well supported by Figures 5a−8a, which show a sharp increase in G_c at $\Sigma_c \approx 0.015$ chains/nm^2. The locus of the final fracture also shifts so that for large Σ, $\Sigma \gg \Sigma_c$, 80% of the dPS is found on the epoxy surface of the fracture for all N's in this regime. The reason for this shift is that for low Σ, the weakest position is near the interface itself. As Σ increases, the dPS chains become more stretched and some disentanglement becomes more likely, so the weakest point shifted toward the tip of the dPS brush. The craze failure mechanism then corresponds to a mixture of chain scission and disentanglement near the interface between the dPS block "brush" and the PS homopolymer matrix of the HIPS.

Pullout to Crazing Transition ($N = 410$). According to fracture mechanism map in Figure 1, at low Σ we should expect to see a transition N^* from pullout of the grafted chains to scission when $\sigma_{pullout} = \sigma_{scission}$ Using $f_{mono}^{HIPS} = 6.3 \times 10^{-2}$ N/mer and $f_b = 2 \times 10^{-9}$ N/bond[12] for eqs 1 and 3, the estimated N^* is approximately 350. Here the static monomer friction of HIPS is taken as $f_{mono}^{HIPS} \approx 6.3 \times 10^{-12}$ N/mer $= f_{mono}^{PVP}$, which is a reasonable value.[5] However, investigations of chain pullout fracture revealed that when $N_e < N < N^*$, there is an extra friction force because of entanglements in addition to the static friction force used to predict N^*.[24] Therefore pure pullout should only occur when $N < N_e$. Using the crazing stress for HIPS obtained above, we would expect to see for $N = 160$ that at $\Sigma^\dagger \approx 0.03$ chains/nm^2 there should be a transition from chain pullout to crazing. But we did not see this transition, and this can be explained by the −COOH being embedded under the epoxy surface, resulting in a much shorter effective chain length. From the data in the previous section, $N' = 220$, the entire $N = 160$ dPS chain will be buried in the epoxy, resulting in a G_c that is the same as that of the bare interface. This is indeed what we observe.

For the longer $N = 410$ chains, the effective chain length is 190. The chain pullout to crazing transition,

calculated using eq 4, should occur at $\Sigma^\dagger \approx 0.025$ chains/nm^2. This transition from pullout to crazing is evident Figure 4a, which shows that G_c is low until $\Sigma^\dagger \approx 0.025$ chains/nm^2 is reached, followed by a rapid increase in G_c for increasing Σ. Figure 4b shows that for low Σ ($\Sigma < \Sigma^\dagger$) all the deuterium after fracture is found on the epoxy side, which clearly shows that chain pullout is the interface failure mechanism under these conditions. The high G_c value when $\Sigma > \Sigma^\dagger$ suggests that a craze is formed. The interface failure mechanism is craze formation, followed by craze failure by disentanglement in the craze fibrils.

Randomly Carboxylated dPS Chains ($N = 700$). With 1% of the phenyl rings randomly functionalized, $N = 700$ gives 1 carboxylic acid group every 100 monomer units, or about 6 acid groups per chain, with an additional acid group at the terminal end of each chain. The interesting question is which of these −COOH groups along the dPS chain will react with the epoxy and whether it is possible that two −COOH groups widely separated on the same dPS chain will react with epoxy forming an anchored loop of dPS that would penetrate into the HIPS.

Our experimental results shown in Figure 11 indicate that such loop formation is not likely. If loops were formed, then the longest possible chain would be half of the original dPS chain length, corresponding to a double chain of length ~350 units. For this chain length, there will be a pullout to crazing transition at Σ around 0.04 chains/nm^2 from the calculation shown before. But Figure 11a shows the transition occurs much earlier.

If we assume one functional group at an average distance of 1/3 the chain length from one end is grafted on epoxy, then there will be two dPS chains penetrating into the HIPS: one has a chain length of ~200 and another a chain length of ~500. If we assume as before that the −COOH reacts at the same distance below the epoxy surface, $N' = 220$, the effective chain length is ~280 for the longer chain. From eq 4 we can calculate that there will be a transition from chain pullout to crazing at $\Sigma^\dagger \approx 0.017$ chains/nm^2. Figure 11b shows when $\Sigma < \Sigma^\dagger$ all the deuterium is on the epoxy side, which means chain pullout is the failure mechanism. When $\Sigma > \Sigma^\dagger$, the deuterium on the epoxy side will decrease and eventually reaches 80%. This means that some chain scission is involved in the craze failure mechanism here. The high G_c value for $\Sigma > \Sigma^\dagger$ indicates that a craze is formed under these conditions.

Figure 13 shows data for the PS/epoxy interface reinforced by the same $N = 700$ random dPS-COOH chains. Now the transition from pullout to crazing changes to $\Sigma^\dagger \approx 0.03$ chains/nm^2 based on eq 4 and the higher PS crazing stress. The results seem to show such a transition at about the correct $\Sigma^\dagger$.

4. Discussion and Conclusions

The Young's modulus of polybutadiene rubber particles in HIPS is 3 orders of magnitude lower than that of the glassy PS matrix. This modulus mismatch leads to a stress concentration at the equator of the particle during mechanical deformation. The presence of the stress concentration can lead to crazes that propagate from particle to particle and hence to crazing throughout a large volume of material, rather than just at the crack tip. Hence the polymer absorbs a large amount of energy during deformation and is toughened. Also the yield stress of HIPS will be much lower than that of

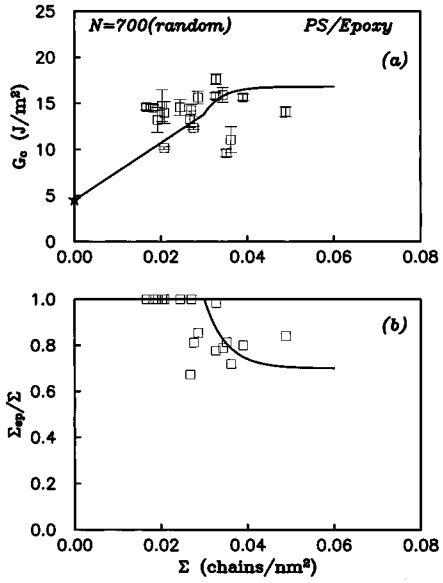

Figure 13. (a) Fracture toughness vs areal chain density for PS/epoxy interface $N = 700$ (random dPS-COOH chain). (b) Fraction of deuterium on epoxy side after fracture for $N = 700$ (random).

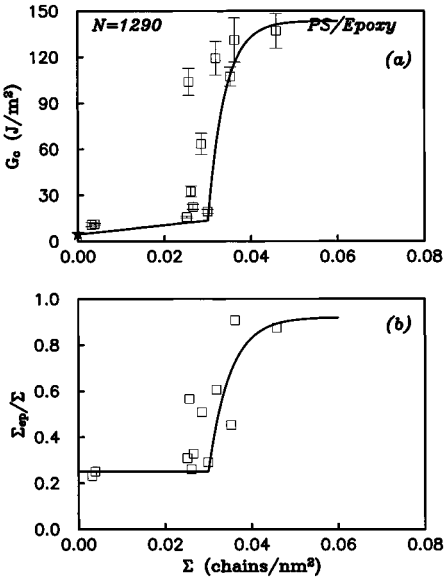

Figure 14. (a) Fracture toughness vs areal chain density for PS/epoxy interface $N = 1290$. (b) Fraction of deuterium remaining on epoxy side after fracture for $N = 1290$.

PS. This is indeed what we observed if we compare our results with the PS/epoxy interface reinforced with the same dPS-COOH polymer chains. Figure 14a shows the G_c vs Σ for the $N = 1290$ dPS chains at the PS/epoxy interface. The G_c is low until an areal chain density $\Sigma \approx 0.03$ chains/nm^2 is reached; then G_c increases rapidly with increasing Σ. The deuterium fraction on the epoxy side after fracture is shown in Figure 14b. The interface fails by chain scission at low Σ, but failure occurs due to craze formation followed by breakdown of the craze at high Σ. This result shows that the chain scission to crazing transition for PS is 0.03 chains/nm^2, in agreement with the value found for PS/epoxy interfaces,[9] and is consistent with the measured crazing stress of PS of about 55 MPa.[12] The crazing stress we obtained for HIPS is ~30 MPa. This shift in crazing stress and transition areal chain density from PS to HIPS is thus as expected.[25]

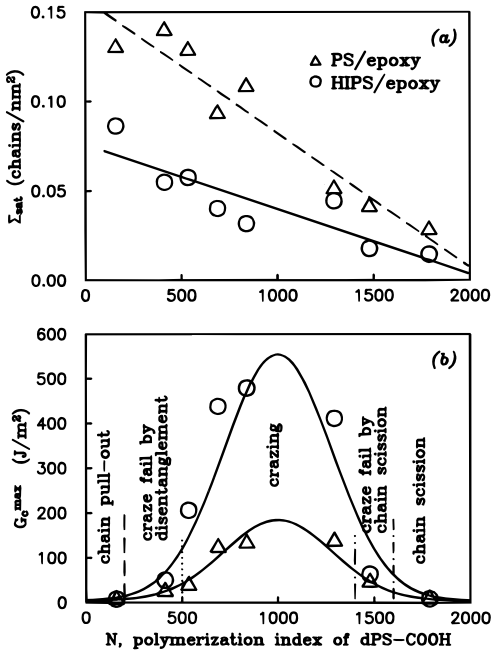

Figure 15. (a) Maximum grafting density as a function of polymerization index N.

Figure 15a shows that the maximum grafting density Σ_{max} of dPS-COOH on the epoxy surface decreases almost linearly with degree of polymerization N. Similar trends were found by Norton et al.[9] for the PS/epoxy system. The Σ_{max} values obtained by Norton et al. are slightly higher than ours. This difference may be due to small differences in sample preparation procedure between the two sets of experiment. A plot of the maximum fracture toughness G_c^{max} (corresponding roughly to the value at Σ_{max}) vs N is shown in Figure 15b. In the low-N region, i.e., $N < 200$, the interface fails by pullout of the dPS without crazing and G_c^{max} is very low. As N increases to 410, a craze can be formed ahead of the crack tip for the largest Σ but this craze fails by chain disentanglement while it is still very narrow. There is a chain pullout to crazing transition at $\Sigma^{\dagger} \approx 0.025$ chains/nm^2 at this chain length. As N is increased still further to 1290, chain scission is the dominant craze failure mechanism, but chain disentanglement still plays a role in craze failure. The interface fails by chain scission at low Σ and craze formation followed by craze breakdown at high Σ. The G_c^{max} can reach as high as 500 J/m^2 for the HIPS/epoxy interface. At $N = 1480$, the craze fails by chain scission but Σ_{max} barely reaches $\Sigma_c \approx 0.015$ chains/nm^2 so the G_c^{max} decreases significantly. Finally, at $N = 1790$, Σ_c cannot be reached and the interface fails by chain scission prior to crazing. To optimize the interface adhesion, a value of N around 1000 appears to be needed, where not much disentanglement will be observed but where relatively large values of the grafting density are still possible.

Acknowledgment. This research was supported by the Materials Science Center at Cornell, which is funded by the National Science Foundation (DMR−MRL program) and benefited from the use of MSC Central Facilities. We would like to thank Dr. Mark Soderquist of the Dow Chemical Company for the specially prepared batch of HIPS.

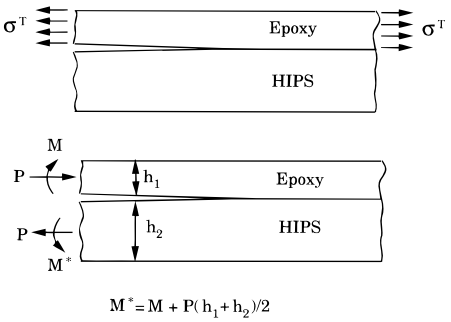

Figure 16. Conversion of the thermal stress problem to one with external loading.

Appendix. Effect of Residual Stresses on G and ψ

The energy release rate G given by eq 5 assumes that the ADCB specimen was in a stress-free state before the razor blade was inserted. This was a good approximation in previous interface fracture experiments where the polymers used, e.g., PS and PVP, PS and PMMA, and PS and epoxy, have very similar thermal expansion coefficients. However, for the epoxy/HIPS system, where the thermal expansion coefficients of epoxy (α_{ep}) and HIPS (α_{hp}), are 65×10^{-6} and 110×10^{-6} K^{-1}, respectively, there should be residual stresses caused by the mismatch of thermal expansion coefficients. These will affect the fracture toughness calculation, particularly for specimens with weak interfaces. So the new energy release rate G^* should be computed by

$$G^* = G + G_T \tag{A1}$$

where G is given by eq 5 and G_T is the contribution due to thermal residual stresses.

The complex stress intensity factor K_r due to thermal expansion coefficient mismatch can be estimated using the result of Suo et al.[26] Let the specimen be bonded in its stress-free state, which is at temperature T_0. Suo et al.[26] showed that the residual stresses in the specimen after cooling to room temperature T are equivalent to the application of loads (P, M) on the specimen as shown in Figure 16. There is a compressive misfit stress between HIPS and epoxy interfaces, which gives rise to a negative value of K_1. The negative K_1 will cause crack surface contact as mentioned in Suo et al.[26] But in our case there is an external razor blade loading which ensures there is no crack surface contact so the K field is still valid. After some simplification of Suo's equations, the force P and torque M defined in Figure 16 are determined to be

$$P = \sigma^T h_{ep}(1 + \Sigma_1 \eta^3)/B \tag{A2}$$

$$M = -\sigma^T h_{ep}{}^2 \Sigma_1 \eta^2 (1 + \eta)/(2B)$$

where $B = 1 + 6\Sigma_1\eta^2 + 4\Sigma_1\eta^3 + 4\Sigma_1\eta + \Sigma_1{}^2\eta^4$. σ^T in eq A2 is the misfit stress and is defined by

$$\sigma^T = \frac{-8\Delta\alpha(T - T_0)(1 - \nu_{ep})}{(\kappa_{ep} + 1)/\mu_{ep}}$$

where $\Delta\alpha = \alpha_{ep} - \alpha_{hp}$. The factor $(1 - \nu_{ep})$ is added to correct for the plane strain condition. The energy release rate G_r due to the thermal loading alone is found to be

$$G_r = \frac{\kappa_{ep}+1}{16\mu_{ep}}\left[\frac{P^2}{Ah_{ep}} + \frac{M^2}{Ih_{ep}} + 2\frac{PM}{(AI)^{1/2}h_{ep}^2}\sin(\gamma)\right] \quad \text{(A3)}$$

The constants A, I, Σ_1, γ, and η in eqs A2 and A3 are defined by

$$A = \frac{1}{1+\Sigma_1(4\eta+6\eta^2+3\eta^3)}$$

$$I = \frac{1}{12(1+\Sigma_1\eta^3)}$$

$$\eta = h_{ep}/h_{hp}$$

$$\sin(\gamma) = 6\Sigma_1\eta^2(1+\eta)(AI)^{1/2}$$

$$\Sigma_1 = \left(\frac{\kappa_{ep}+1}{\mu_{ep}}\right)\Big/\left(\frac{\kappa_{hp}+1}{\mu_{hp}}\right) \quad \text{(A4)}$$

respectively. ν, Poisson's ratio, for both epoxy and HIPS is about 0.34 so $\Sigma_1 \approx E_{ep}/E_{hp}$.

The complex stress intensity factor K_r due to thermal residual stresses is found using eqs A3 and 6a, i.e.

$$K_r = K_{1r} + iK_{2r} = \frac{\cosh(\pi\epsilon)}{(1+\Sigma_1)^{1/2}}\left(\frac{P}{(Ah_{ep})^{1/2}} - ie^{i\gamma}\frac{M}{(Ih_{ep}^3)^{1/2}}\right)h_{ep}^{-i\epsilon}e^{i\omega} \quad \text{(A5)}$$

The real dimensionless quantity ω is a function of the phase angle ψ_r and is tabulated by Suo et al.[26] for different material and geometry combinations.

The actual K field in the specimen is found by superposition, i.e.

$$K = K_1 + iK_2 = K_0 + K_r = (K_{1r} + K_{10}) + i(K_{2r} + K_{20}) \quad \text{(A6)}$$

where $K_0 = K_{10} + iK_{20}$ is the complex stress intensity factor due to the razor blade loading of a specimen without residual stresses. K_0 is given by

$$K_0 = K_{10} + iK_{20} = 4\cosh(\pi\epsilon)\sqrt{G/C}e^{i\psi_0}d^{-i\epsilon} \quad \text{(A7)}$$

where G is given by eq 5 and ψ_0 is the phase angle of the crack tip field in a specimen without residual stresses and is $-16°$ when d is chosen to be 100 μm. Using eq 6a, the actual energy release rate G^* is found to be

$$G^* = G + G_r + \frac{G^{1/2}}{2}\left(\frac{\kappa_{ep}+1}{\mu_{ep}}\right)^{1/2} \times \left[\frac{P}{(Ah_{ep})^{1/2}}\cos(\varphi) + \frac{M}{(Ih_{ep}^3)^{1/2}}\sin(\varphi+\gamma)\right] \quad \text{(A8)}$$

where $\varphi = \omega - \epsilon\ln(h_1) - \psi_0 + \epsilon\ln(d)$ and G_r is given by eq A3. G_T in eq A1 is determined by the last two terms in eq A8, i.e.

$$G_T = G_r + \frac{G^{1/2}}{2}\left(\frac{\kappa_{ep}+1}{\mu_{ep}}\right)^{1/2} \times \left[\frac{P}{(Ah_{ep})^{1/2}}\cos(\varphi) + \frac{M}{(Ih_{ep}^3)^{1/2}}\sin(\varphi+\gamma)\right] \quad \text{(A9)}$$

References and Notes

(1) Fayt, R.; Jérôme, R.; Teyssié, P. *J. Polym. Sci., Polym. Lett. Ed.* **1981**, *19*, 79.
(2) Lindsey, C. R.; Paul, D. R.; Barlow, J. W. *J. Appl. Polym. Sci.* **1981**, *26*, 1.
(3) Fayt, R.; Jérôme, R.; Teyssié, Ph. *J. Polym. Sci., Polym. Phys. Ed.* **1982**, *2*, 2209.
(4) Xiao, F.; Hui, C. Y.; Washiyama, J.; Kramer, E. J. *Macromolecules* **1994**, *27*, 4382.
(5) Washiyama, J.; Kramer, E. J.; Hui, C. Y. *Macromolecules* **1993**, *26*, 2928.
(6) Dai, K. H.; Kramer, E. J.; Fréchet, J. M. J.; Wilson, P. G.; Long, T. E. *Macromolecules* **1994**, *27*, 5187.
(7) Xu, Z.; Kramer, E. J.; Lochmann, L.; Fréchet, J. M. J., to be submitted for publication.
(8) Lee, Y.; Char, K. *Macromolecules* **1994**, *27*, 2603.
(9) Norton, L. J.; Smigolova, V.; Pralle, M. U.; Hubenko, A.; Dai, K. H.; Kramer, E. J.; Hahn, S.; Berglund, C.; DeKoven, B. *Macromolecules* **1995**, *28*, 1999.
(10) Kramer, E. J.; Norton, L. J.; Dai, C. A.; Sha, Y.; Hui, C. Y. *Faraday Discuss.* −1994, *98*/8.
(11) Brown, H. R. *J. Mater. Sci.* **1990**, *25*, 2791.
(12) Creton, C.; Kramer, E. J.; Hui, C. Y.; Brown, H. R. *Macromolecules* **1992**, *25*, 3075. Creton, C. Ph.D. Thesis, Cornell University, Ithaca, NY, 1992.
(13) Xiao, F.; Hui, C. Y.; Kramer, E. J. *J. Mater. Sci.* **1993**, *28*, 5620.
(14) Xu, D. B.; Hui, C. Y.; Kramer, E. J.; Creton, C. *Mech. Mater.* **1991**, *11*, 257.
(15) Hird, B.; Eisenberg, A. *J. Polym. Sci., Part A: Polym. Chem.* **1993**, *31*, 1377.
(16) Calistri-Yeh, M.; Kramer, E. J.; Sharma, R.; Zhao, W.; Rafailovich, M. H.; Sokolov, J.; Brock, J. D. *Langmuir*, in press.
(17) Kramer, E. J. *Isr. J. Chem.* **1995**, *35*, 49.
(18) Rice, J. R. *J. Appl. Mech.* **1988**, *55*, 98.
(19) Rice, J. R.; Sih, G. C. *J. Appl. Mech.* **1965**, *32*, 418.
(20) Erdogan, F. *J. Appl. Mech.* **1965**, *32*, 403.
(21) By analogy to what happens in the PS/PVP system,[4] we expect that positive values of ψ result in crazes being nucleated from the interface well ahead of the crack tip and growing into the HIPS on a plane making an angle of about 45° to the direction of crack growth along the interface. These crazes widen as the crack approaches, leading to an increased G_c.
(22) *Encyclopeida of Polymer Science and Engineering*, 2nd ed.; John Wiley & Sons: New York, 1984; Vol. 16, p 737.
(23) Onogi, S.; Masuda, T.; Kitagawa, K. *Macromolecules* **1970**, *3*, 109.
(24) Washiyama, J.; Kramer, E. J.; Creton, C.; Hui, C. Y. *Macromolecules* **1994**, *27*, 2019.
(25) Bucknall, C. B.; Davies, P.; Partridge, I. K. *J. Mater. Sci.* **1987**, *22*, 1341.
(26) Suo, Z.; Hutchinson, *Int. J. Fract.* **1990**, *43*, 1.

MA951794I